LETTER

Dendritic cells control lymphocyte entry to lymph nodes through high endothelial venules

Christine Moussion[1,2] & Jean-Philippe Girard[1,2]

While patrolling the body in search of foreign antigens, naive lymphocytes continuously circulate from the blood, through the lymph nodes, into the lymphatic vessels and back to the blood[1,2]. This process, called lymphocyte recirculation, provides the body with effective immune surveillance for foreign invaders and for alterations to the body's own cells. However, the mechanisms that regulate lymphocyte recirculation during homeostasis remain incompletely characterized. Here we show that dendritic cells (DCs), which are well known for their role in antigen presentation to T lymphocytes[3], control the entry of naive lymphocytes to lymph nodes by modulating the phenotype of high endothelial venules (HEVs), which are blood vessels specialized in lymphocyte recruitment[2,4,5]. We found that *in vivo* depletion of CD11c^{+} DCs in adult mice over a 1-week period induces a reduction in the size and cellularity of the peripheral and mucosal lymph nodes. In the absence of DCs, the mature adult HEV phenotype reverts to an immature neonatal phenotype, and HEV-mediated lymphocyte recruitment to lymph nodes is inhibited. Co-culture experiments showed that the effect of DCs on HEV endothelial cells is direct and requires lymphotoxin-β-receptor-dependent signalling. DCs express lymphotoxin, and DC-derived lymphotoxin is important for lymphocyte homing to lymph nodes *in vivo*. Together, our results reveal a previously unsuspected role for DCs in the regulation of lymphocyte recirculation during immune surveillance.

Lymphocyte entry to lymph nodes is initiated by the lymphocyte homing receptor L-selectin, which mediates lymphocyte rolling along HEV walls[2,4–6]. In contrast to the endothelium that lines other vessels, HEV endothelial cells in lymph nodes have a plump, almost cuboidal morphology[4,5], and they express high levels of sulphated carbohydrate ligands for L-selectin, which are recognized by the monoclonal antibody MECA-79 (refs 6–9) and are synthesized by the HEV-specific enzymes GlcNAc6ST-2 (a sulphotransferase)[8,9] and FucT-VII (a fucosyltransferase)[10]. Studies carried out in rodents have shown that, when the peripheral lymph nodes (PLNs) are deprived of afferent lymph, the HEVs lose their characteristics and their ability to support lymphocyte traffic[11–14]. Together with data obtained from human studies[15], these results indicate that the lymphoid tissue microenvironment is crucial for the maintenance of HEV characteristics during homeostasis[4,15]. However, the cell types involved have not been defined.
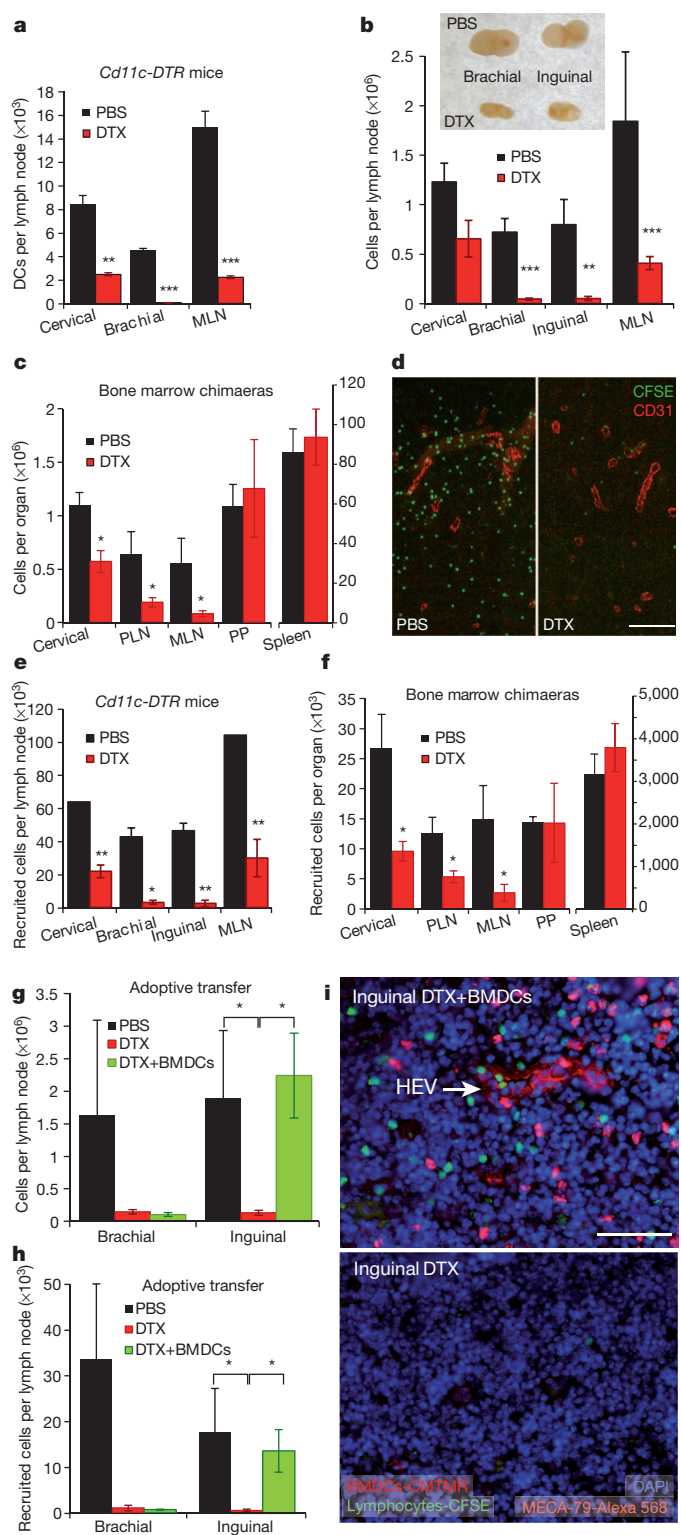
To address the potential role of DCs in the maintenance of HEVs, we took advantage of the CD11c–diphtheria toxin receptor (*Cd11c-DTR*) transgenic mouse model[16], which allows *in vivo* depletion of CD11c^{+} DCs in adult mice after treatment with diphtheria toxin (DTX). Because downregulation of the HEV phenotype occurs 1 week after occlusion of the afferent lymphatics[12], we decided to deplete the DCs over 1 week by injecting DTX every 2 days (Fig. 1a and Supplementary Fig. 1). After 8 days of DC depletion, we observed a reduction in the size and cellularity of all lymph nodes that were analysed, with the most striking effects in the PLNs (the brachial and inguinal lymph nodes) and the mesenteric lymph nodes (Fig. 1b). By contrast, the number of leukocytes and lymphocytes in

the blood was not significantly altered by DC depletion (Supplementary Fig. 2). We observed weight loss after repeated DTX treatment of *Cd11c–DTR* mice (Supplementary Fig. 3a), as previously reported[16,17]. These deleterious effects of DTX are thought to result from the expression of the DTR on non-haematopoietic radioresistant cells[17]. To confirm our initial observations, we therefore generated bone marrow chimaeras in which *Cd11c-DTR* expression was restricted to the haematopoietic compartment[17]. Lethally irradiated wild-type mice were reconstituted with bone marrow from *Cd11c-DTR* transgenic mice, and 3 months later, they were treated with DTX for 10 days, without any adverse side effects (Supplementary Fig. 3a). The total cellularity in the lymph nodes was reduced in DTX-treated chimaeric mice, whereas the cellularity in the Peyer's patches and the spleen was not affected (Fig. 1c). By contrast, we observed no significant changes in the cellularity of the lymph nodes after prolonged DTX treatment of lethally irradiated *Cd11c-DTR* transgenic mice that had been reconstituted with wild-type bone marrow (Supplementary Fig. 3b, c), despite these mice rapidly succumbing to weight loss and death, as previously described[17].

To determine whether the reduced cellularity in the absence of DCs results from inhibition of lymphocyte entry to lymph nodes, we next performed short-term homing assays. The homing of lymphocytes from the blood to the PLNs and mucosal lymph nodes was strongly reduced in DTX-treated *Cd11c-DTR* transgenic and chimaeric mice compared with PBS-treated mice (Fig. 1d–f). The effects of DC depletion on lymphocyte homing and lymph node cellularity in *Cd11c-DTR* chimaeric mice were completely reversible after DTX injections were stopped (Supplementary Fig. 4). In addition, we found that adoptive transfer of wild-type, bone-marrow-derived CD11c^{+} DCs (wild-type BMDCs; Supplementary Fig. 5) to DTX-treated *Cd11c-DTR* transgenic mice could recover the normal cellularity of, and the homing of naive lymphocytes to, the draining lymph nodes (Fig. 1g, h). The adoptively transferred CD11c^{+} BMDCs were located around HEVs expressing antigens recognized by MECA-79 (denoted MECA-79^{+} HEVs) in the draining lymph nodes (Fig. 1i), and *Ccr7^{−/−}* BMDCs had a lower capacity than wild-type BMDCs to recover lymph node cellularity and homing to lymph nodes (Supplementary Fig. 5). Together, these results indicate that CD11c^{+} DCs are essential for lymphocyte homing to lymph nodes (Supplementary Discussion).

We next analysed the HEV phenotype and observed a marked downregulation of HEV-specific markers (FucT-VII, GlcNAc6ST-2 and the L-selectin counter receptor GLYCAM1 (ref. 6), as well as MECA-79 antigens) in the PLNs of DC-depleted mice (Fig. 2a and Supplementary Fig. 6). By contrast, the expression of pan-endothelial cell markers, such as CD31 (also known as PECAM1), was unaffected (Fig. 2a). Strikingly, the expression of MADCAM1, a marker of immature neonatal HEVs[18], was induced on the blood vessels in the inguinal lymph nodes of DC-depleted mice (Fig. 2a). Thus, *in vivo* depletion of CD11c^{+} DCs induces specific changes in HEV phenotype, with a reversion from the mature adult HEV phenotype (MECA-79^{hi}GLYCAM1^{hi}FucT-VII^{hi}GlcNAc6ST-2[hi]MADCAM1^{lo}) to the immature HEV phenotype

[1]CNRS, Institut de Pharmacologie et de Biologie Structurale, 205 route de Narbonne, F-31077 Toulouse, France. [2]Université de Toulouse, UPS, Institut de Pharmacologie et de Biologie Structurale, F-31077 Toulouse, France.
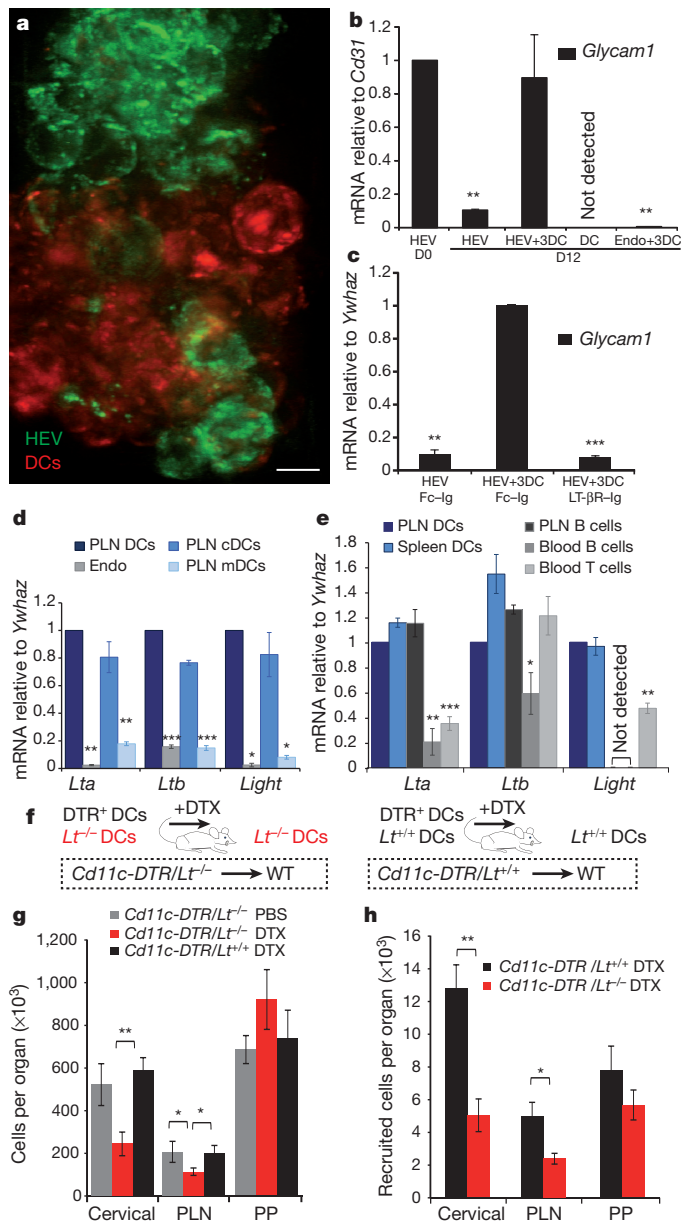
MECA-79$^+$ cells was also reduced (by ~75%), it was nevertheless possible to isolate these cells by flow cytometry. Analysis of HEV-specific gene expression by reverse transcription followed by quantitative PCR (RT–qPCR) showed that expression of the HEV-specific genes *Glycam1*, *FucT-VII* (also known as *Fut7*) and *GlcNAc6ST2* (also known as *Chst4*) was strongly reduced after DTX treatment, whereas the expression of the genes encoding the pan-endothelial cell markers CD31 and VE-cadherin was not downregulated after depletion of DCs (Fig. 2b). The expression of several other genes involved in the multi-step lymphocyte adhesion cascade (*Ccl21*, *Icam1*, *Cxcl13* and *Vcam1*) was also not altered in DC-depleted mice (Supplementary Fig. 8). Therefore, CD11c$^+$ DCs are essential for the maintenance of HEV-specific gene expression.

We then analysed lymphocyte–HEV interactions in the inguinal lymph nodes from *Cd11c-DTR* chimaeric mice by using intravital microscopy. As previously described[19], the HEV phenotype is found only in venular orders III to V (Fig. 3a), which support the bulk of lymphocyte trafficking to lymph nodes. The rolling fraction of wild-type lymphocytes in venular orders II to V was not significantly different between *Cd11c-DTR* chimaeric mice that had been treated with DTX and those treated with PBS (Fig. 3b). However, the fraction of lymphocytes that transitioned from primary rolling to secondary firm adhesion (the sticking fraction) was markedly decreased in HEVs (orders III to V) from DC-depleted mice (Fig. 3c). In addition, the rolling velocity of lymphocytes in HEVs was significantly increased (Fig. 3d, e). For instance, the median rolling velocity of lymphocytes in order IV HEVs increased from 20 μm s^{-1} in PBS-treated mice to 92 μm s^{-1} in DTX-treated mice. Thus, *in vivo* depletion of CD11c$^+$ DCs in *Cd11c-DTR* chimaeric mice elicited considerable alterations in lymphocyte rolling velocity and lymphocyte sticking inside lymph node HEVs.

An important question raised by our observations is whether CD11c$^+$ DCs regulate HEV phenotype directly or through other cell types that are found in the lymph nodes. Analyses in *Rag2$^{-/-}$* mice and *Rag2$^{-/-}$ Cd11c-DTR* transgenic mice showed that lymphocytes are not essential for the homeostatic maintenance of HEV phenotype and that the effects of CD11c$^+$ DCs on lymphocyte homing occur in the absence of T and B lymphocytes (Supplementary Fig. 9). Therefore, we next considered the possibility that DCs, which are strategically positioned close to HEV walls *in vivo*[20,21], may regulate HEV phenotype directly. We developed a co-culture model of MECA-79$^+$CD31$^+$ HEV endothelial cells with CD11c$^+$MHC class II$^+$ DCs (Fig. 4a), both of which were isolated from the PLNs of wild-type mice (Supplementary Fig. 10).

Setting up the culture conditions for the purified HEV endothelial cells turned out to be technically challenging because these cells were available in a limited quantity (constituting 0.02% of total lymph node cells) and nothing was known about the conditions required to maintain the cells *ex vivo*. We eventually found that culture of the purified HEV endothelial cells on plates coated with fibronectin and type I collagen in an appropriate endothelial/DC culture medium allowed the survival of the cells *ex vivo* for at least 12 days. However, HEV-specific gene

(MECA-79^{lo}GLYCAM1^{lo}FucT-VII^{lo}GlcNAc6ST-2^{lo}MADCAM1^{hi}), which is found in PLNs at birth[13,14,18] or after the occlusion of the afferent lymphatics[12–14].

To determine whether the changes in HEV phenotype occur at the RNA level, we purified MECA-79$^+$CD31$^+$ HEV and MECA-79$^-$CD31$^+$ non-HEV endothelial cells from the PLNs of *Cd11c-DTR* transgenic mice that had been treated with DTX or PBS (Supplementary Fig. 7). Although the percentage of MECA-79$^+$ cells in the CD31$^+$ endothelial cell population was halved after DTX treatment, and the intensity of MECA-79 staining on the remaining

Figure 2 | CD11c+ DCs are essential for the homeostatic maintenance of HEV phenotype. a, PLN sections from control mice (control) or *Cd11c-DTR* transgenic mice (DTX) treated with DTX for 8 days were stained with MECA-79 or antibodies specific for the indicated proteins (left). Quantitative image analysis of the immunofluorescence staining is also shown (right). Scale bar, 100 μm. **b**, qPCR analysis was performed using total RNA from HEV endothelial cells (HEV) and non-HEV endothelial cells (Endo) that were sorted by flow cytometry after isolation from DTX-treated or PBS-treated *Cd11c-DTR* transgenic mice. The mean and s.d. from triplicate qPCR runs are plotted. Data are representative of three independent experiments. *, $P < 0.05$; ***, $P < 0.001$.

expression (as determined by measuring the levels of *Glycam1* messenger RNA) was strongly reduced when HEV endothelial cells were grown alone *ex vivo* (Fig. 4b). Strikingly, when MECA-79+ HEV endothelial cells were co-cultured with CD11c+ DCs purified from

Figure 3 | CD11c+ DCs control the rolling velocity and firm adhesion of lymphocytes inside PLN HEVs. a, Visualization of the inguinal lymph node microcirculation by intravital microscopy. **b–e**, The rolling fraction (**b**), sticking fraction (**c**) and cumulative rolling velocities (**d, e**) of fluorescently labelled wild-type lymphocytes were determined in the indicated venules. Data were collected from three DTX- and three PBS-treated *Cd11c-DTR* bone marrow chimaeras. **d, e**, Data represent the percentages of cells rolling at or below a given velocity (V_{roll}). The median V_{roll} in order III venules was 62.5 μm s^{-1} in PBS-treated chimaeras and 129.6 μm s^{-1} in DTX-treated chimaeras (**d**). The median V_{roll} in order IV venules was 20.3 μm s^{-1} in PBS-treated chimaeras and 92.9 μm s^{-1} in DTX-treated chimaeras (**e**). (**d**, PBS, $n = 22$ cells, 5 venules and 3 mice; DTX, $n = 20$ cells, 6 venules and 3 mice; **e**, PBS, $n = 12$ cells, 4 venules and 3 mice; DTX, $n = 22$ cells, 10 venules and 3 mice.) Error bars, s.e.m. *, $P < 0.05$; ***, $P < 0.001$.

wild-type mice, *Glycam1* mRNA levels were maintained at levels similar to those found in HEVs that were freshly purified from the PLNs (Fig. 4b and Supplementary Fig. 11), indicating that CD11c+ DCs regulate HEV phenotype directly. *FucT-VII* and *GlcNAc6ST-2* mRNA levels could not be quantified in these experiments, probably because our qPCR assay was not sensitive enough or because all of the properties of HEVs may not be maintained in the co-cultures.

The lymphotoxin-β receptor (LT-βR), which is expressed on HEV endothelial cells[22], has been shown to have a crucial role in the homeostatic maintenance of HEVs[23], so we tested the possibility that this receptor may be involved in the cross-talk between HEV endothelial cells and CD11c+ DCs. We found that interrupting LT-βR signalling through the addition of LT-βR–immunoglobulin soluble inhibitor (but not control Fc–immunoglobulin) to the co-cultures abrogated the enhancing effect of CD11c+ DCs on *Glycam1* expression *ex vivo* (Fig. 4c and Supplementary Fig. 11). CD11c+ DCs isolated from the PLNs (Supplementary Fig. 10) or the spleen expressed transcripts encoding the LT-βR ligands lymphotoxin-α (LT-α), LT-β and LIGHT (Fig. 4d, e), and the expression levels of these ligands were higher in CD11c^hi^MHC class II^med^ DCs (classical DCs (cDCs); the major population depleted in *Cd11c-DTR* transgenic mice) than in CD11c^med^MHC class II^hi^ DCs (migratory DCs (mDCs)) (Fig. 4d). Interestingly, the expression levels of LT-α- and LT-β-encoding transcripts (*Lta* and *Ltb* mRNA) in DCs were similar to those of naive B cells from PLNs (Fig. 4e), and such levels are sufficient for the maintenance of follicular DC networks in the lymph nodes[24]. The expression levels of *Lta* and *Ltb* in DCs may thus be appropriate for homeostatic maintenance of HEVs.

Figure 4 | DC-derived LT is important for lymphocyte homing to lymph nodes *in vivo*. a, Immunofluorescence staining of HEVs (MECA-79 staining) co-cultured with DCs. Scale bar, 10 μm. **b–e**, qPCR analysis of *Glycam1* (**b**, **c**), *Lta*, *Ltb* and *Light* (**d**, **e**) mRNA levels. Mean and s.d. from triplicate qPCR runs are plotted (**b–e**). D, day; Endo, non-HEV endothelial cells; HEV+3DC (Endo+3DC), the number of DCs in the co-cultures was threefold the number of HEV (Endo) endothelial cells. **f–h**, Analysis of *Cd11c-DTR/Lt*^{−/−} and *Cd11c-DTR/Lt*^{+/+} chimaeric mice (**f**). Lethally irradiated wild-type (WT) mice were reconstituted with the indicated bone marrow mixture (dashed boxes). Cellularity in (**g**) and lymphocyte homing to (**h**) lymph nodes were determined by flow cytometry after 10 days of DTX treatment (*n* = 4 mice per group). Data are representative of two independent experiments. **b–e**, **g**, **h**, Error bars, s.e.m. *, *P* < 0.05; **, *P* < 0.01; ***, *P* < 0.001.

To examine the potential role of DC-derived LT *in vivo*, we generated mixed bone marrow chimaeras by reconstituting lethally irradiated wild-type mice with 50% bone marrow from *Cd11c-DTR* transgenic mice and 50% bone marrow from *Lta*-deficient (denoted *Lt*^{−/−}) or wild-type (*Lt*^{+/+}) mice (Fig. 4f). Injection of DTX into the *Cd11c-DTR/Lt*^{−/−} or *Cd11c-DTR/Lt*^{+/+} chimaeric mice induced depletion of *Lt*^{+/+} DCs harbouring the *Cd11c-DTR* transgene but spared non-transgenic *Lt*^{−/−} and *Lt*^{+/+} DCs (Supplementary Fig. 12). The cellularity of the PLNs and cervical lymph nodes and lymphocyte homing to these lymph nodes (Fig. 4g, h), but not to the Peyer's patches

and the spleen (Supplementary Fig. 12), were significantly reduced in DTX-treated *Cd11c-DTR/Lt*^{−/−} chimaeric mice (which retained only LT-deficient CD11c^{+} DCs) compared with DTX-treated *Cd11c-DTR/Lt*^{+/+} chimaeric mice. DC-derived LT is thus important *in vivo* for HEV-mediated lymphocyte recruitment to lymph nodes.

In conclusion, our findings uncover a previously unsuspected and important function of DCs in the control of HEV phenotype and lymphocyte entry to lymph nodes during homeostasis in adult mice. DCs thus have a dual role; they function as antigen-presenting cells[3], but they also regulate lymphocyte recirculation to ensure that the appropriate lymphocytes will come into contact with their cognate antigens. The role of DCs in the maintenance of blood vessel phenotype is reminiscent of the role of astrocytes in the brain[4,25]. However, astrocytes induce blood–brain barrier characteristics that limit the entry of molecules and cells (including lymphocytes) to the brain, whereas DCs regulate HEV characteristics that allow lymphocyte entry to lymph nodes. The development of HEVs is observed in many chronic inflammatory diseases[4], and CD11c^{+} DCs from inflamed tissues produce LT[26,27] and regulate HEV angiogenesis[28]. A better understanding of the cross-talk between DCs and HEVs may thus provide a basis for novel approaches to control the development of HEVs in clinical situations.

METHODS SUMMARY

Cd11c-DTR mice (B6.FVB-Tg[Itgax-DTR/EGFP.57]Lan/J) were purchased from the EMMA European network, and C57BL/6 mice were purchased from Charles River Laboratories. C57BL/6:*Lt*^{−/−} mice were provided by H. Korner and S. A. Nedospasov. For bone marrow chimaeras, a single-cell suspension generated from the flushed bone marrow of femurs and tibias was injected intravenously into mice that had been irradiated with 900 rad. Chimaeras were incubated for at least 12 weeks before use. All mice were handled according to institutional guidelines under protocols approved by the Institut de Pharmacologie et de Biologie Structurale and Région Midi-Pyrénées animal care committees. For DC depletion, mice were treated with DTX (Sigma), which was administered intraperitoneally at 6 ng per gram (body weight) every two days. BMDCs were generated in medium containing mouse GM-CSF, as described previously[29], and then treated with lipopolysaccharide and injected subcutaneously into recipient mice every 2 days. Homing assays and intravital microscopy analyses with fluorescent lymphocytes were performed as previously described[19,20]. Immunofluorescence staining was performed on Bouin-fixed, paraffin-embedded or cryopreserved mouse lymph node sections. HEV endothelial cells (CD45^{−}CD31^{+}MECA-79^{+}) and non-HEV endothelial cells (CD45^{−}CD31^{+}MECA-79^{−}) were isolated from lymph node stromal-cell suspensions (using pooled PLNs from 5–20 mice) by flow cytometry using a FACSAria II cell sorter. CD11c^{+}MHC class II^{+} wild-type DCs were sorted from non-adherent cells in the same pool of PLN cells. For co-culture assays, sorted cells were seeded in 96-well tissue culture plates coated with rat fibronectin, type I collagen and gelatine (Sigma) and were grown *ex vivo* for 11–12 days in endothelial/DC culture medium. LT-βR–immunoglobulin fusion protein (5 μg ml^{−1}; R&D Systems) or control human Fc–immunoglobulin was added to the co-cultures every 2 days. qPCR was performed as described previously[30]. Statistical analysis was performed using the Mann–Whitney test (for lymph node cellularity and velocity histograms) or an unpaired Student's *t*-test (for homing assays, and rolling and sticking fractions). Differences were considered statistically significant when *P* < 0.05.

Full Methods and any associated references are available in the online version of the paper at www.nature.com/nature.

1. Butcher, E. C. & Picker, L. J. Lymphocyte homing and homeostasis. *Science* **272,** 60–66 (1996).
2. von Andrian, U. H. & Mempel, T. R. Homing and cellular traffic in lymph nodes. *Nature Rev. Immunol.* **3,** 867–878 (2003).
3. Banchereau, J. & Steinman, R. M. Dendritic cells and the control of immunity. *Nature* **392,** 245–252 (1998).
4. Girard, J. P. & Springer, T. A. High endothelial venules (HEVs): specialized endothelium for lymphocyte migration. *Immunol. Today* **16,** 449–457 (1995).
5. Miyasaka, M. & Tanaka, T. Lymphocyte trafficking across high endothelial venules: dogmas and enigmas. *Nature Rev. Immunol.* **4,** 360–370 (2004).
6. Rosen, S. D. Ligands for L-selectin: homing, inflammation, and beyond. *Annu. Rev. Immunol.* **22,** 129–156 (2004).

7. Streeter, P. R., Rouse, B. T. & Butcher, E. C. Immunohistologic and functional characterization of a vascular addressin involved in lymphocyte homing into peripheral lymph nodes. *J. Cell Biol.* **107,** 1853–1862 (1988).

8. Uchimura, K. *et al.* A major class of L-selectin ligands is eliminated in mice deficient in two sulfotransferases expressed in high endothelial venules. *Nature Immunol.* **6,** 1105–1113 (2005).

9. Kawashima, H. *et al. N*-acetylglucosamine-6-*O*-sulfotransferases 1 and 2 cooperatively control lymphocyte homing through L-selectin ligand biosynthesis in high endothelial venules. *Nature Immunol.* **6,** 1096–1104 (2005).

10. Malý, P. *et al.* The α(1,3)fucosyltransferase Fuc-TVII controls leukocyte trafficking through an essential role in L-, E-, and P-selectin ligand biosynthesis. *Cell* **86,** 643–653 (1996).

11. Hendriks, H. R. & Eestermans, I. L. Disappearance and reappearance of high endothelial venules and immigrating lymphocytes in lymph nodes deprived of afferent lymphatic vessels: a possible regulatory role of macrophages in lymphocyte migration. *Eur. J. Immunol.* **13,** 663–669 (1983).

12. Mebius, R. E., Streeter, P. R., Breve, J., Duijvestijn, A. M. & Kraal, G. The influence of afferent lymphatic vessel interruption on vascular addressin expression. *J. Cell Biol.* **115,** 85–95 (1991).

13. Swarte, V. V. *et al.* Regulation of fucosyltransferase-VII expression in peripheral lymph node high endothelial venules. *Eur. J. Immunol.* **28,** 3040–3047 (1998).

14. Mebius, R. E. *et al.* Expression of GlyCAM-1, an endothelial ligand for L-selectin, is affected by afferent lymphatic flow. *J. Immunol.* **151,** 6769–6776 (1993).

15. Lacorre, D. A. *et al.* Plasticity of endothelial cells: rapid dedifferentiation of freshly isolated high endothelial venule endothelial cells outside the lymphoid tissue microenvironment. *Blood* **103,** 4164–4172 (2004).

16. Jung, S. *et al. In vivo* depletion of CD11c+ dendritic cells abrogates priming of CD8+ T cells by exogenous cell-associated antigens. *Immunity* **17,** 211–220 (2002).

17. Zaft, T., Sapoznikov, A., Krauthgamer, R., Littman, D. R. & Jung, S. CD11chigh dendritic cell ablation impairs lymphopenia-driven proliferation of naive and memory CD8+ T cells. *J. Immunol.* **175,** 6428–6435 (2005).

18. Mebius, R. E., Streeter, P. R., Michie, S., Butcher, E. C. & Weissman, I. L. A developmental switch in lymphocyte homing receptor and endothelial vascular addressin expression regulates lymphocyte homing and permits CD4+ CD3− cells to colonize lymph nodes. *Proc. Natl Acad. Sci. USA* **93,** 11019–11024 (1996).

19. Von Andrian, U. H. Intravital microscopy of the peripheral lymph node microcirculation in mice. *Microcirculation* **3,** 287–300 (1996).

20. Bajenoff, M., Granjeaud, S. & Guerder, S. The strategy of T cell antigen-presenting cell encounter in antigen-draining lymph nodes revealed by imaging of initial T cell activation. *J. Exp. Med.* **198,** 715–724 (2003).

21. Mempel, T. R., Henrickson, S. E. & Von Andrian, U. H. T-cell priming by dendritic cells in lymph nodes occurs in three distinct phases. *Nature* **427,** 154–159 (2004).

22. Liao, S. & Ruddle, N. H. Synchrony of high endothelial venules and lymphatic vessels revealed by immunization. *J. Immunol.* **177,** 3369–3379 (2006).

23. Browning, J. L. *et al.* Lymphotoxin-β receptor signaling is required for the homeostatic control of HEV differentiation and function. *Immunity* **23,** 539–550 (2005).

24. Ansel, K. M. *et al.* A chemokine-driven positive feedback loop organizes lymphoid follicles. *Nature* **406,** 309–314 (2000).

25. Janzer, R. C. & Raff, M. C. Astrocytes induce blood–brain barrier properties in endothelial cells. *Nature* **325,** 253–257 (1987).

26. GeurtsvanKessel, C. H. *et al.* Dendritic cells are crucial for maintenance of tertiary lymphoid structures in the lung of influenza virus-infected mice. *J. Exp. Med.* **206,** 2339–2349 (2009).

27. Muniz, L. R., Pacer, M. E., Lira, S. A. & Furtado, G. C. A critical role for dendritic cells in the formation of lymphatic vessels within tertiary lymphoid structures. *J. Immunol.* **187,** 828–834 (2011).

28. Webster, B. *et al.* Regulation of lymph node vascular growth by dendritic cells. *J. Exp. Med.* **203,** 1903–1913 (2006).

29. Lutz, M. B. *et al.* An advanced culture method for generating large quantities of highly pure dendritic cells from mouse bone marrow. *J. Immunol. Methods* **223,** 77–92 (1999).

30. Cayrol, C. *et al.* The THAP-zinc finger protein THAP1 regulates endothelial cell proliferation through modulation of pRB/E2F cell-cycle target genes. *Blood* **109,** 584–594 (2007).

Author Contributions C.M. designed the study, performed all of the experiments and analysed the data. J.-P.G. designed the study, analysed the data and wrote the paper.

Author Information Reprints and permissions information is available at www.nature.com/reprints. The authors declare no competing financial interests. Readers are welcome to comment on the online version of this article at www.nature.com/nature. Correspondence and requests for materials should be addressed to J.-P.G. (Jean-Philippe.Girard@ipbs.fr).

METHODS

Mice. C57BL/6 wild type mice were purchased from Charles River Laboratories, and *Cd11c-DTR* transgenic mice (B6.FVB-Tg$^{Itgax-DTR/EGFP.57}$Lan/J)[16] were purchased from the EMMA European network. *Cd11c-DTR* mice were maintained on the C57BL/6 and C57BL/6:*Rag2*$^{-/-}$ genetic backgrounds. All *CD11c*-DTR transgenic mice used in this study were heterozygous transgenic. C57BL/6:*Lt*$^{-/-}$ mice[31,32] were provided by H. Korner and S. A. Nedospasov. C57BL/6:*Cd45.1* and C57BL/6:*Rag2*$^{-/-}$ mice were obtained from O. Lantz, and C57BL/6:*Ccr7*$^{-/-}$ mice were obtained from M. Lipp and E. Donnadieu. All mice were bred under specific-pathogen-free conditions and handled according to institutional guidelines under protocols approved by the Institut de Pharmacologie et de Biologie Structurale and Région Midi-Pyrénées animal care committees.

Bone marrow chimaeras. A single-cell suspension generated from the flushed bone marrow of femurs and tibias from donor mice was injected intravenously into mice that had been irradiated with 900 rad. Chimaeras were incubated for at least 12 weeks before use. Mixed bone marrow chimaeras[33] were generated by transferring a mixture of 50% bone marrow from *Cd11c-DTR* transgenic mice and 50% bone marrow from *Lt*$^{+/+}$ or *Lt*$^{-/-}$ mice into lethally irradiated wild-type recipient mice.

Depletion of CD11c$^+$ DCs. For systemic DC depletion, mice were given DTX (Sigma) intraperitoneally at a dose of 6 ng per gram (body weight) every two days. As controls, mice received intraperitoneal injections of PBS vehicle. *Cd11c-DTR* transgenic and chimaeric mice were treated with DTX or PBS for 8 and 10 days, respectively. To evaluate the efficacy of DC depletion, spleens and lymph nodes were analysed by flow cytometry for the presence of CD11c$^+$GFP$^+$ cells or CD11c$^+$MHC class II$^+$ cells.

Analysis of blood and lymph nodes. Peripheral blood was obtained by cardiac puncture and was stored in EDTA-containing tubes at 4 °C until analysis with an automated haematological analyser (Sysmex XT 2000i). Freshly isolated mucosal lymph nodes (three cervical and one mesenteric) and PLNs (one inguinal and one brachial) were digested with type D collagenase (Roche laboratories), and single-cell suspensions were counted (size >7 µm) with a Z1 Particle Counter (Beckman Coulter).

Analysis of surface markers. The following monoclonal antibodies for cell surface staining were purchased from BD Biosciences: anti-CD11c (HL3), anti-CD45.1 (A20), anti-CD45.2 (104), anti-Gr1 (RB6-8C5), anti-CD3 molecular complex (17A2) and anti-CD19 (1D3) antibodies. The following monoclonal antibodies were purchased from eBioscience: anti-CD11c (N418) and anti-MHC class II (I–A/I–E) (M5/114.15.2) antibodies. After a 20-min blocking step on ice (in PBS containing 1% FCS, 5% normal mouse serum, 5 mM EDTA, 0.1% NaN$_3$, 5 µg ml^{-1} anti-CD16/CD32 (2.4G2, BD Biosciences)), cells were incubated with conjugated antibodies (conjugates were FITC, Alexa 488, PE, PE-Cy7, Alexa 700, biotin or APC) diluted in FACS buffer (PBS containing 1% FCS, 5 mM EDTA and 0.1% NaN$_3$). When biotinylated monoclonal antibodies were used, cells were incubated with APC- or PE-Cy7-conjugated streptavidin (BD Biosciences). Flow cytometry analyses were performed on a FACSCalibur or an LSRII flow cytometer (BD Biosciences).

Immunofluorescence staining. Immunofluorescence staining was performed on 5 µm sections from Bouin-fixed, paraffin-embedded or cryopreserved mouse lymph nodes, as described previously[34], using the following primary antibodies: the rat monoclonal antibodies MECA-79 (ATCC) and MECA-367 (anti-MADCAM1, Pharmingen; for cryosections); rabbit polyclonal antibodies against CD31 (Abcam), GLYCAM1 (CAM02; provided by S. D. Rosen), GlcNAc6ST-2 (GST-3, provided by S. D. Rosen) and FucT-VII (provided by J. B. Lowe). For quantitative image analysis of the immunofluorescence staining, lymph node sections were immunostained in parallel using the same dilutions of antibodies and reagents, and fluorescent images, which were captured using identical exposure times and settings, were analysed with ImageJ software, as described previously[35].

***In vivo* homing assays.** A single-cell suspension of naive lymphocytes was prepared from a pool of spleen (after lysis of the red blood cells in ammonium chloride, potassium bicarbonate and EDTA) and PLNs from C57BL/6 mice. Lymphocytes labelled with CFSE (Molecular Probes, Invitrogen) were injected intravenously into recipient mice. The number of fluorescent cells recruited to each lymph node was determined 4 h after injection, by flow cytometry or by fluorescence microscopy, as described previously[20].

Adoptive transfer of BMDCs. BMDCs were generated in medium containing mouse GM-CSF, as described previously[29]. BMDCs were then incubated with 0.5 µg ml^{-1} lipopolysaccharide (Sigma-Aldrich) for 1 h at 37 °C, washed, labelled with CMTMR (Molecular Probes, Invitrogen) and injected (5 × 10^6 cells per mouse) into two subcutaneous sites (the footpad and thigh). Cells were injected every 2 days at the time of intraperitoneal DTX injection, for 8 days (a total of 2 × 10^7 BMDCs per mouse). In some experiments, BMDCs were prepared in the absence of lipopolysaccharide (Supplementary Fig. 5d, e).

Intravital microscopy. Intravital microscopy was performed as described previously[19,36,37]. Naive lymphocytes labelled with calcein (Molecular Probes, Invitrogen) were injected into the right femoral artery, and cell behaviour in lymph node venules was assessed as described previously[19]. To determine the rolling fractions (the percentage of rolling cells in the total flux of cells in each venule) and the sticking fractions (the percentage of rolling cells that subsequently arrested for >30 s), the data were generated from three DTX-treated *Cd11c-DTR* chimaeric mice (number of venules analysed/venular order: 2/II, 4/III, 8/IV and 16/V) and three PBS-treated *Cd11c-DTR* chimaeric mice (number of venules analysed/venular order: 2/II, 3/III, 5/IV and 7/V) (with DTX and PBS treatment for 10 days). In some experiments, Alexa-488-conjugated MECA-79 monoclonal antibody (Molecular probes A488 labelling kit) was injected intravenously to visualize the HEV network.

Isolation of HEV endothelial cells and CD11c$^+$MHC class II$^+$ DCs from PLNs. PLNs were pooled and gently squeezed, and the non-adherent cells were washed out. The stromal elements were digested with type II collagenase (Gibco) for 1 h at 37 °C, and the single-cell suspensions obtained were passed through a 40 µm cell strainer (BD Biosciences) and stained with anti-CD45 (30-F11, BD Biosciences), anti-CD31 (MEC13.3, BD Biosciences) and MECA-79 monoclonal antibodies for 1 h at 4 °C. In some experiments, one round of CD45$^+$ cell depletion with Dynabeads was performed. HEV endothelial cells (CD45$^-$CD31$^+$MECA-79$^+$) and non-HEV endothelial cells (CD45$^-$CD31$^+$MECA-79$^-$) were isolated by cell sorting using a FACSAria II cell sorter (BD Biosciences). CD11c$^+$MHC class II$^+$ wild-type DCs, CD11c^{hi}MHC class II^{med} DCs (classical DCs (cDCs)) and CD11c^{med}MHC class II^{hi} DCs (migratory DCs (mDCs)) were sorted from non-adherent cells from the same PLNs. Anti-rat/hamster Igκ chain compensation particles (BD CompBeads, BD Biosciences), single stained with each of the antibodies, were used as compensation controls.

Co-culture assays. Sorted cells were seeded in 96-well tissue culture plates coated with rat fibronectin (Sigma) and type I collagen (Sigma) in 0.2% gelatine (Sigma). Cells were grown *ex vivo* for 11–12 days in endothelial/DC culture medium: a mixture of 50% BD Endothelial Cell Culture Medium and 50% RPMI-1640 supplemented with 1× Endothelial Cell Growth Supplement (ECGS, BD Biosciences), 1× epidermal growth factor (EGF, BD Biosciences), 15% FCS, 8% mouse serum, L-glutamine, non-essential amino acids, penicillin/streptomycin (Invitrogen), 10 ng ml^{-1} recombinant mouse GM-CSF (tebu-bio) and 2-mercaptoethanol (Sigma). Survival of the isolated HEV endothelial cells in culture was sensitive to the batches of ECGS and serum; in some experiments, 1.5× ECGS, 1.5× EGF, 20% FCS, 4% newborn calf serum and 4% KnockOut Serum Replacement (Invitrogen) were used to increase the survival of the cells. In some experiments, LT-βR–immunoglobulin fusion protein (5 µg ml^{-1}, R&D Systems) or control human Fc–immunoglobulin (5 µg ml^{-1}, Chemicon) was added to the co-cultures every 2 days.

qPCR. Total RNA was isolated from DCs, HEV endothelial cells and non-HEV endothelial cells with an Absolutely RNA Nanoprep kit (Stratagene), and qPCR was performed as described previously[30]. The housekeeping gene *Ywhaz* and the endothelial cell gene *Cd31* were used as control genes for normalization. The primer sequences were as follows: *Ywhaz*, 5′-ACTTTTGGTACATTGTGGCTT CAA-3′ and 5′-CCGCCAGGACAAACCAGTAT-3′; *Cd31*, 5′-TCCCTGGGAG GTCGTCCAT-3′ and 5′-GAACAAGGCAGCGGGGTTTA-3′; VE-cadherin, 5′-TCCTCTGCATCCTCACTATCACA-3′ and 5′-GTAAGTGACCAACTGCT CGTGAAT-3′; *Glycam1*, 5′-AGAATCAAGAGGCCCAGGAT-3′ and 5′-TGG GTCTTGTGGTCTCTTCCA-3′; *FucT-VII*, 5′-CAGATGCACCCTCTAGTACT CTGG-3′ and 5′-TGCACTGTCCTTCCACAACC-3′; *GlcNAc6ST2*, 5′-GGCA AGCAGAAGGGTTAGG-3′ and 5′-CTGGGAACCCAGGAACATC-3′; *Ltb*, 5′-ACCTCATAGGCGCTTGGATG-3′ and 5′-ACGCTTCTTCTTGGCTCGC-3′; *Lta*, 5′-CCAGGACAGCCCATCCACT-3′ and 5′-GTACCCAACAAGGTGAGC AGC-3′; *Light*, 5′-CGATCTCACCAGGCCAAC-3′ and 5′-TCCACCAATACCT ATCAAGCTG-3′; *Ccl21*, 5′-AAGGCAGTGATGGAGGGG-3′ and 5′-CGGG TAAGAACAGGATTG-3′; *Cxcl13*, 5′-CATAGATCGGGATTCAAGTTACG-3′ and 5′-TCTTGGTCCAGATCACAACTTCA-3′; *Icam1*, 5′-GGGAATGTCAC CAGGAATGT-3′ and 5′-GCACCAGAATGATTATAGTCCA-3′; *Vcam1*, 5′-GGATCGCTCAAATCGGGTGA-3′ and 5′-GGTGACTCGCAGCCCGTA-3′; and *Gapdh*, 5′-CCACCCCAGCAAGGACACT-3′ and 5′-GAAATTGTGAGGG AGATGCTCA-3′.

Statistical analysis. Statistical analysis was performed using the Mann–Whitney test (for lymph node cellularity and velocity histograms) or an unpaired Student's *t*-test (for homing assays, and rolling and sticking fractions). For BMDC adoptive transfer, PBS and DTX groups were compared with a Mann–Whitney test, and DTX and DTX+BMDC groups were compared with a paired Student's *t*-test. Differences were considered statistically significant when $P < 0.05$.

31. Körner, H. *et al.* Distinct roles for lymphotoxin-α and tumor necrosis factor in organogenesis and spatial organization of lymphoid tissue. *Eur. J. Immunol.* **27**, 2600–2609 (1997).

32. Kuprash, D. V. *et al.* Redundancy in tumor necrosis factor (TNF) and lymphotoxin (LT) signaling *in vivo*: mice with inactivation of the entire TNF/LT locus versus single-knockout mice. *Mol. Cell. Biol.* **22,** 8626–8634 (2002).
33. Sapoznikov, A. *et al.* Perivascular clusters of dendritic cells provide critical survival signals to B cells in bone marrow niches. *Nature Immunol.* **9,** 388–395 (2008).
34. Moussion, C., Ortega, N. & Girard, J. P. The IL-1-like cytokine IL-33 is constitutively expressed in the nucleus of endothelial cells and epithelial cells *in vivo*: a novel 'alarmin'? *PLoS ONE* **3,** e3331 (2008).
35. Chen, Q. *et al.* Fever-range thermal stress promotes lymphocyte trafficking across high endothelial venules via an interleukin 6 *trans*-signaling mechanism. *Nature Immunol.* **7,** 1299–1308 (2006).
36. Carriere, V. *et al.* Cancer cells regulate lymphocyte recruitment and leukocyte–endothelium interactions in the tumor-draining lymph node. *Cancer Res.* **65,** 11639–11648 (2005).
37. Flaishon, L. *et al.* Anti-inflammatory effects of an inflammatory chemokine: CCL2 inhibits lymphocyte homing by modulation of CCL21-triggered integrin-mediated adhesions. *Blood* **112,** 5016–5025 (2008).